ASYMMETRY IN LOW-RANK ADAPTERS OF FOUNDATION MODELS

Anonymous authors
Paper under double-blind review

ABSTRACT

Parameter-efficient fine-tuning optimizes large, pre-trained foundation models by updating a subset of parameters; in this class, Low-Rank Adaptation (LoRA) is particularly effective. Inspired by an effort to investigate the different roles of LoRA matrices during fine-tuning, this paper characterizes and leverages unexpected asymmetry in the importance of low-rank adapter matrices. Specifically, when updating the parameter matrices of a neural network by adding a product BA, we observe that the B and A matrices have distinct functions: A extracts features from the input, while B uses these features to create the desired output. Based on this observation, we demonstrate that fine-tuning B is inherently more effective than fine-tuning A and that a random untrained A should perform nearly as well as a fine-tuned one. Using an information-theoretic lens, we also bound generalization of low-rank adapters, showing that the parameter savings of exclusively training B improves the bound. We support our conclusions with experiments on RoBERTa, BART, LLaMA-2, and ViT.

1 INTRODUCTION

Foundation models for data-rich modalities like text and imagery have achieved significant success by pre-training large models on vast amounts of data. While these models are designed to be general-purpose, it is often necessary to *fine-tune* them for downstream tasks. The huge size of foundation models, however, can make fine-tuning the entire model impossible, inspiring parameter-efficient fine-tuning (PEFT) methods that selectively update fewer parameters (c.f. Lialin et al., 2023). PEFT's effectiveness demonstrates that updating even a tiny fraction of the parameters can retain or enrich the capabilities of pretrained models, and has become a necessary ingredient, e.g., the PEFT package (HuggingFace, Year) has been supporting more than 4.4k projects since its creation in November 2022.

Among PEFT methods, low-rank adaptation (LoRA) (Hu et al., 2021) has become increasingly popular, leveraging an assumption that over-parameterized models have a low intrinsic dimension (Aghajanyan et al., 2021). To update a neural network, LoRA trains a subset of the parameters (usually attention) by representing weight matrices as $W_0 + \Delta W$, where W_0 is the fixed weight matrix form the pre-trained model and ΔW is a low-rank update. Compared to full fine-tuning, LoRA considerably reduces the number of trainable parameters and memory requirements and often achieves similar or better performance.

Most LoRA implementations factor $\Delta W = BA$ and optimize for A and B, where A and B have fewer rows and columns (resp.) than ΔW; this is the approach proposed by Hu et al. (2021). With this set of variables, the standard LoRA training procedure—wherein A is initialized to a random matrix and B is initialized to zero—reflects a curious asymmetry, which is leveraged in some empirical follow-ups (Zhang et al., 2023a; Kopiczko et al., 2024). In particular, while training B is critical for the performance of LoRA, even a *randomly* initialized A seems to suffice for strong performance. Reversing the roles of A and B substantially decreases performance.

Digging into this empirical suggestion from prior work, this paper shows that LoRA's components are inherently asymmetric. In fact, the asymmetry occurs even for linear models (§B.1.1). Indeed, our theoretical (§B) and empirical analysis (§C) suggests that fixing A to a random orthogonal matrix can yield similar performance to full LoRA training, and that this adjustment may even promote

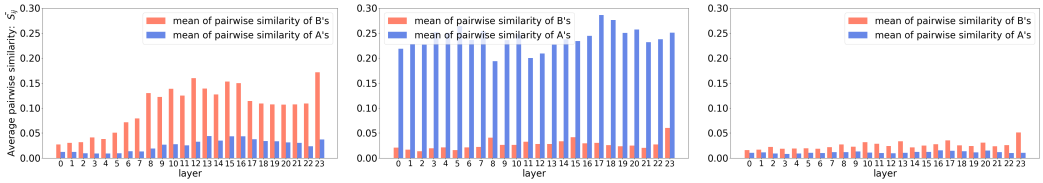

(a) Random initialization, same task (b) Fixed initialization, different tasks (c) Random initialization, different tasks

Figure 1: Similarity of learned LoRA matrices A & B across layers of a RoBERTa model fine-tuned with different initialization and data settings. The experiment demonstrates the asymmetric roles of A and B in LoRA. A detailed discussion is in **motivating example**.

generalization. This observation is backed by a comprehensive empirical study, leading to practical suggestions for improving parameter efficiency and generalization of LoRA models.

Contributions. Our contributions are as follows: (1) We provide simple theoretical and empirical analysis demonstrating *asymmetry* of training the two adapter matrices, showing that tuning B is more impactful than tuning A. This confirms and builds on prior empirical observations (Zhang et al., 2023a; Kopiczko et al., 2024). (2) We show theoretically and empirically that randomly drawing and freezing A while tuning only B can improve generalization vs. tuning both B and A, in addition to practical gains achieved by $2\times$ parameter reduction. (3) We validate our findings through experiments using models including RoBERTa, BART-Large, Llama-2, and the vision transformer (ViT).

2 Preliminaries & Background

Motivating example. In Figure 1, we investigate the similarity of learned matrices A and B under three scenarios: (a) random initialization, A & B trained multiple times on the same task; , (b) fixed initialization, A & B trained multiple times, each time on a different task; and (c) random initialization, A & B trained multiple times, each time on a different task. Here, we fine-tune RoBERTa large (Liu et al., 2019) with LoRA on the tasks from the GLUE benchmark (Wang et al., 2018). Specifically, we fine-tuned *mrpc* with 5 random seeds for (a) and on *mrpc, rte, stsb, and cola* for (b) and (c). The figure plots similarity of learned A and B matrices across layers in Figure 1, measured by canonical correlation analysis goodness of fit (Ramsay et al., 1984); see Appendix D for motivation. These plots suggest that B is predominantly responsible for learning, while A is less important. Specifically, when training on the same task with different initializations (scenario (a)), the learned B matrices are similar to each other, while when training on different tasks (scenarios (b) and (c)), they are different. On the contrary, the similarity of learned A matrices is insensitive to training data and is determined by initialization; it is highest in scenario (b) when the initialization is fixed even though training data differs.

3 Theoretical Analysis Results

In this section, we show the results of the theoretical analysis of the asymmetry in prediction tasks and its effect on generalization. A complete analysis is presented in the appendix.

We discuss a general case rather than a specific neural network architecture, considering rank r adaptation of any parameter matrix $W = W_0 + BA$ used multiplicatively on some input-dependent vector, i.e.,

$$\text{layerOutput} = \psi((W_0 + BA) \cdot \phi(\text{layerInput}), \dots) \tag{1}$$

for some differentiable functions ψ, ϕ. Here, ψ may take more arguments depending on layerInput, which may have their own low rank adapted parameter matrices. This generic form encompasses both feedforward and attention layers.

In this setting, A serves to extract r features from $\phi(\text{layerInput})$, which are then used by B to predict some desired output for future layers. We will argue that training B to predict the output is crucial for correct outputs, while using a random A is often sufficient, as B can be optimized to use whatever information is retained in the r-dimensional projection $A \cdot \phi(\text{layerInput})$.

3.1 A, B ASYMMETRY IN PREDICTION TASKS

If we wish to reduce the effort of training both A and B in (3), in principle either A could be frozen and B tuned or B frozen and A tuned. As shown in §C and elsewhere, these two options are not empirically equivalent: It is best to freeze A and tune B. In this section, we seek to understand the principle behind this asymmetry by theoretically analyzing the fine-tuning of a class of prediction models. We first build intuition with least-squares linear regression.

3.1.1 MULTIVARIATE LINEAR LEAST-SQUARES

As a simple example analogous to a single network layer, we study d_{in}-to-d_{out} least-squares linear regression (in (3), set ϕ, ψ to be identity). Specifically, suppose there is an input $X \in \mathbb{R}^{d_{in}}$, an output $Y \in \mathbb{R}^{d_{out}}$, and a pre-trained linear model

$$y_{pre}(X) = W_0 X + b_0,$$

where $W_0 \in \mathbb{R}^{d_{out} \times d_{in}}$ and $b_0 \in \mathbb{R}^{d_{out}}$. With this model held constant, our goal is regressing (Y_{targ}, X_{targ}) pairs where Y_{targ} is given by: $Y_{targ} = W_{targ} X_{targ} + b_{targ}$ with $W_{targ} = W_0 + \Delta$. Following LoRA, we model the target Δ using a low rank update to the pre-trained W_0, i.e. $W = W_0 + BA$: $\hat{y}(x) = (W_0 + BA)x + b$, where $B \in \mathbb{R}^{d_{out} \times r}$ and $A \in \mathbb{R}^{r \times d_{in}}$ for some r.

To find an A and B that best matches the output, we optimize the least squares loss on the difference between $\hat{y}$ and Y_{targ}:

$$\mathcal{L}(A, B) = \mathbb{E}_{(Y_{targ}, X_{targ})}[\|Y_{targ} - (W_0 + BA)X_{targ} - b\|_2^2]. \tag{2}$$

Below, we present lemmas on minimizing this loss while freezing either A or B. In both, for simplicity, we set $b = b_{targ}$ and $\mathbb{E}[X_{targ}] = 0$ and defer proofs to Appendix E.

Lemma 3.1 (Freezing A yields regression on projected **features**). *Optimizing $\mathcal{L}(A, B)$ while fixing $A = Q$ with $QQ^\top = I_r$ yields*

$$B^* = \Delta \Sigma Q^\top (Q \Sigma Q^\top)^{-1},$$

where $\Sigma = \mathrm{Cov}[X_{targ}]$, with expected loss $\mathcal{L}(Q, B^*) = d_{out}\sigma^2 + \mathrm{Tr}[\Delta \Sigma \Delta^\top] - \mathrm{Tr}[Q \Sigma \Delta^\top \Delta \Sigma Q^\top (Q \Sigma Q^\top)^{-1}]$.

Lemma 3.2 (Freezing B yields regression on projected **outputs**). *Optimizing $\mathcal{L}(A, B)$ while fixing $B = U$ with $U^\top U = I_r$ yields*

$$A^* = U^\top (W_{targ} - W_0),$$

with expected loss $\mathcal{L}(A^*, U) = d_{out}\sigma^2 + \mathrm{Tr}[\Delta \Sigma \Delta^\top] - \mathrm{Tr}[U^\top \Delta \Sigma \Delta^\top U]$, where $\Sigma = \mathrm{Cov}[X_{targ}]$.

Comparing the lemmas above, A^* is simply the U projection of the targeted change in weight matrix $\Delta = W_{targ} - W_0$. Unlike B^*, the optimal choice of A^* does not consider the input data distribution captured by Σ.

Intuitively, if the goal of adaptation is to approximate some desired output, then projecting away the majority (since $r \ll d_{out}$) of the output is undesirable. In contrast, projecting away a portion of the input feature space will be less damaging, if the information X_{targ} contains about Y_{targ} is redundant (c.f., neuron dropout (Srivastava et al., 2014) in neural network training) or if the distribution of X_{targ} tends to be low-rank. We validate the above intuition with the following theorem:

Theorem 3.3 (A, B output fit asymmetry). *Consider the settings of Lemmas 3.1 and 3.2, and suppose U, Q are sampled uniformly from their respective Stiefel manifolds. Then, $\mathcal{L}(A^*, U) \geq \mathcal{L}(Q, B^*)$ with high probability as $d/r \to \infty$.*

In other words, the least-squares prediction loss of only fine-tuning B is at least as good as only fine-tuning A. Moreover, in the appendix we further show the performance advantage of tuning B over A is large when $d \gg r$, which is the typical regime in practice.

Based on our above result, we extend our theoretical analysis to §B.1.2 nonlinear losses and multilayer models. Also, we show the advantages of tuning only B matrix (§B.2) including parameter efficiency (§B.2.1) and provable better generalization (§B.2.2). In sum, our analysis characterizes the different roles of A and B matrix. Our theory shows that just fine-tuning B while freezing A corresponds to learning projected feature space, and should yield better performance than freezing B. Next, our experimental results will verify our understanding across multiple models and datasets.

Table 1: Different adaptation methods on the GLUE benchmark.

Model & Method	# Trainable Parameters	MNLI	SST-2	MRPC	CoLA	QNLI	RTE	STS-B	Avg.
LoRA ($r = 8$)	0.8%	$90.3_{\pm.07}$	$95.6_{\pm0.36}$	$90.3_{\pm0.85}$	$64.4_{\pm1.8}$	$94.0_{\pm0.29}$	$84.1_{\pm0.96}$	$91.5_{\pm0.16}$	87.2
AdaLoRA	2.5%	$90.4_{\pm.37}$	$95.9_{\pm.13}$	$90.1_{\pm.54}$	$67.5_{\pm1.3}$	$94.7_{\pm.22}$	$85.4_{\pm.20}$	$91.3_{\pm1.0}$	87.9
$(IA)^3$	0.7%	$90.0_{\pm.21}$	$95.4_{\pm.17}$	$83.7_{\pm.13}$	$57.6_{\pm.67}$	$93.7_{\pm.07}$	$70.3_{\pm1.5}$	$87.0_{\pm0.4}$	82.5
LoRA-FA	0.3%	$90.3_{\pm.06}$	$95.6_{\pm.17}$	$90.6_{\pm.32}$	$67.3_{\pm2.3}$	$93.4_{\pm.61}$	$82.4_{\pm1.4}$	$91.2_{\pm.29}$	87.3
$\hat{\mathbf{B}}_0 A_{rand}$ ($r = 8$)	0.3%	$90.1_{\pm.19}$	$\underline{95.8}_{\pm.29}$	$89.7_{\pm.13}$	$\underline{\mathbf{67.5}}_{\pm\mathbf{1.2}}$	$\underline{94.0}_{\pm.27}$	$82.8_{\pm1.5}$	$\underline{\mathbf{91.9}}_{\pm\mathbf{.26}}$	87.4
$\hat{\mathbf{B}}_0 A_{rand}$ ($r = 16$)	0.8%	$90.1_{\pm.20}$	$\underline{\mathbf{96.1}}_{\pm\mathbf{.18}}$	$\underline{\mathbf{90.7}}_{\pm\mathbf{.90}}$	$66.1_{\pm2.6}$	$\underline{\mathbf{94.4}}_{\pm\mathbf{.10}}$	$\underline{\mathbf{84.1}}_{\pm\mathbf{.96}}$	$91.2_{\pm.42}$	87.5
$B_{rand}\hat{\mathbf{A}}_0$ ($r = 8$)	0.3%	$\underline{\mathbf{90.3}}_{\pm\mathbf{.18}}$	$95.5_{\pm.66}$	$89.3_{\pm.09}$	$58.7_{\pm2.5}$	$93.8_{\pm.21}$	$77.1_{\pm1.3}$	$90.7_{\pm.31}$	84.2
$B_{rand}\hat{\mathbf{A}}_0$ ($r = 16$)	0.8%	$89.9_{\pm.19}$	$\underline{95.6}_{\pm.64}$	$90.2_{\pm0.23}$	$60.3_{\pm3.3}$	$93.9_{\pm0.25}$	$80.4_{\pm0.21}$	$90.9_{\pm0.13}$	85.9

Method	# Param.	XSum	CNN/DailyMail
$\hat{\mathbf{B}}_0 A_{rand,r=16}$	0.44 %	**42.91 / 19.61 / 34.64**	**43.65 / 20.62 / 40.72**
$B_{rand}\hat{\mathbf{A}}_{0,r=16}$	0.44 %	42.37 / 19.30 / 34.29	43.38 / 20.36 / 40.48
$\hat{\mathbf{B}}_0 \hat{\mathbf{A}}_{rand,r=8}$	0.44 %	43.78 / **20.47** / **35.53**	43.96 / 20.94 / 41.00
$\hat{\mathbf{B}}_{rand}\hat{\mathbf{A}}_{0,r=8}$	0.44 %	**43.80** / 20.39 / 35.48	**44.07 / 21.08 / 41.19**

Table 2: R-1/2/L (%) on text summarization with BART-large on XSum and CNN/DailyMail.

Method	# Param.	0-shot Hums	STEM	Social	Other	Avg
Llama-2-7B	100%	34.22	29.58	34.64	35.60	34.93
LoRA $_{r=32}$	0.24%	40.12	33.92	43.21	**45.21**	40.56
$\hat{\mathbf{B}}_0 A_{rand,r=32}$	0.12%	**44.17**	**36.00**	**46.88**	45.14	**43.01**
$B_{rand}\hat{\mathbf{A}}_{0,r=32}$	0.12%	35.72	31.13	42.05	41.24	37.75

Table 3: 0-shot accuracy (%) on the MMLU benchmark.

4 EXPERIMENTS

We investigate the asymmetry of low-rank adaptation methods with RoBERTa (Liu et al., 2019), BART (Lewis et al., 2020), Llama-2 (Touvron et al., 2023), and Vistion Transformer (Dosovitskiy et al., 2020). We evaluate the performance of fine-turning strategies on natural language understanding (GLUE (Wang et al., 2018), MMLU (Hendrycks et al., 2020)), natural language generation (XSum (Narayan et al., 2018) and CNN/DailyMail (Chen et al., 2016)), and multi-domain image classification (Gulrajani & Lopez-Paz, 2020). The details of experimental results, including implementation, baselines, and analysis are in the appendix.

Using the General Language Understanding Evaluation (GLUE, Wang et al., 2018) benchmark (Table 1), we can see a clear trend where solely updating the B matrix outperforms just learning the A matrix. In addition, when doubling the rank to match the trainable parameters, $\hat{\mathbf{B}}_0 A_{orth}$ consistently outperforms conventional LoRA. We can also observe similar asymmetry in natural language summarization task (Table 4) and the more complicated MMLU benchmark (Table 4) where we fine-tune a Llama-2-7b model (Touvron et al., 2023). In addition, only updating matrix B generally results in better out-of-domain test accuracy when fine-tuning the Vision Transformer model on multidomain image classification task (DomainBed (Gulrajani & Lopez-Paz, 2020), (Table 7)).

5 CONCLUSION

In this paper, we formally identify and investigate asymmetry in the roles of low-rank adapter matrices in LoRA fine-tuning. The A matrices extract features from the input, while the B matrices project these features towards the desired objective.

We illustrate differences between the two matrices from both theoretical and empirical perspectives. Our theoretical analysis explains asymmetry in the fine-tuning of large models. Our theoretical findings further suggests that freezing A as a random orthogonal matrix can improve generalization, a claim we corroborate with experiments across multiple models and datasets.

Our work serves as an initial step to unveil the mechanisms of fine-tuning large models. Our interpretation of low-rank adapters provides an understanding that can benefit future research directions, promoting efficiency and interpretability in foundational models.

REFERENCES

Armen Aghajanyan, Sonal Gupta, and Luke Zettlemoyer. Intrinsic dimensionality explains the effectiveness of language model fine-tuning. In *Proceedings of the 59th Annual Meeting of the Association for Computational Linguistics and the 11th International Joint Conference on Natural Language Processing (Volume 1: Long Papers)*. Association for Computational Linguistics, 2021. doi: 10.18653/v1/2021.acl-long.568. URL http://dx.doi.org/10.18653/v1/2021.acl-long.568.

Nadav Benedek and Lior Wolf. Prilora: Pruned and rank-increasing low-rank adaptation. 2024. URL https://api.semanticscholar.org/CorpusID:267068991.

Danqi Chen, Jason Bolton, and Christopher D. Manning. A thorough examination of the cnn/daily mail reading comprehension task. In *Proceedings of the 54th Annual Meeting of the Association for Computational Linguistics (Volume 1: Long Papers)*. Association for Computational Linguistics, 2016. doi: 10.18653/v1/p16-1223. URL http://dx.doi.org/10.18653/v1/P16-1223.

Tim Dettmers, Artidoro Pagnoni, Ari Holtzman, and Luke Zettlemoyer. Qlora: Efficient finetuning of quantized llms. *ArXiv*, abs/2305.14314, 2023. URL https://api.semanticscholar.org/CorpusID:258841328.

Alexey Dosovitskiy, Lucas Beyer, Alexander Kolesnikov, Dirk Weissenborn, Xiaohua Zhai, Thomas Unterthiner, Mostafa Dehghani, Matthias Minderer, Georg Heigold, Sylvain Gelly, Jakob Uszkoreit, and Neil Houlsby. An image is worth 16x16 words: Transformers for image recognition at scale, 2020.

Jonathan Frankle and Michael Carbin. The lottery ticket hypothesis: Finding sparse, trainable neural networks, 2018.

Amir Gholami, Sehoon Kim, Zhen Dong, Zhewei Yao, Michael W. Mahoney, and Kurt Keutzer. A survey of quantization methods for efficient neural network inference, 2021.

Ishaan Gulrajani and David Lopez-Paz. In search of lost domain generalization, 2020.

Han Guo, Philip Greengard, Eric P. Xing, and Yoon Kim. Lq-lora: Low-rank plus quantized matrix decomposition for efficient language model finetuning, 2024.

Ligong Han, Yinxiao Li, Han Zhang, Peyman Milanfar, Dimitris Metaxas, and Feng Yang. Svdiff: Compact parameter space for diffusion fine-tuning. *arXiv preprint arXiv:2303.11305*, 2023.

Dan Hendrycks, Collin Burns, Steven Basart, Andy Zou, Mantas Mazeika, Dawn Song, and Jacob Steinhardt. Measuring massive multitask language understanding, 2020.

J. Edward Hu, Yelong Shen, Phillip Wallis, Zeyuan Allen-Zhu, Yuanzhi Li, Shean Wang, and Weizhu Chen. Lora: Low-rank adaptation of large language models. *ArXiv*, abs/2106.09685, 2021. URL https://api.semanticscholar.org/CorpusID:235458009.

HuggingFace. Peft. https://github.com/huggingface/peft, Year.

Soroush Abbasi Koohpayegani, KL Navaneet, Parsa Nooralinejad, Soheil Kolouri, and Hamed Pirsiavash. Nola: Networks as linear combination of low rank random basis, 2023.

Dawid J. Kopiczko, Tijmen Blankevoort, and Yuki M. Asano. Vera: Vector-based random matrix adaptation, 2024.

Simon Kornblith, Mohammad Norouzi, Honglak Lee, and Geoffrey Hinton. Similarity of neural network representations revisited. In *International conference on machine learning*, pp. 3519–3529. PMLR, 2019.

Ananya Kumar, Aditi Raghunathan, Robbie Jones, Tengyu Ma, and Percy Liang. Fine-tuning can distort pretrained features and underperform out-of-distribution, 2022.

Mike Lewis, Yinhan Liu, Naman Goyal, Marjan Ghazvininejad, Abdelrahman Mohamed, Omer Levy, Veselin Stoyanov, and Luke Zettlemoyer. Bart: Denoising sequence-to-sequence pre-training for natural language generation, translation, and comprehension. In *Proceedings of the 58th Annual Meeting of the Association for Computational Linguistics*. Association for Computational Linguistics, 2020. doi: 10.18653/v1/2020.acl-main.703. URL http://dx.doi.org/10.18653/v1/2020.acl-main.703.

Vladislav Lialin, Vijeta Deshpande, and Anna Rumshisky. Scaling down to scale up: A guide to parameter-efficient fine-tuning. *arXiv preprint arXiv:2303.15647*, 2023.

Chin-Yew Lin. Rouge: A package for automatic evaluation of summaries. In *Text summarization branches out*, pp. 74–81, 2004.

Haokun Liu, Derek Tam, Mohammed Muqeeth, Jay Mohta, Tenghao Huang, Mohit Bansal, and Colin A Raffel. Few-shot parameter-efficient fine-tuning is better and cheaper than in-context learning. *Advances in Neural Information Processing Systems*, 35:1950–1965, 2022.

Weiyang Liu, Zeju Qiu, Yao Feng, Yuliang Xiu, Yuxuan Xue, Longhui Yu, Haiwen Feng, Zhen Liu, Juyeon Heo, Songyou Peng, Yandong Wen, Michael J. Black, Adrian Weller, and Bernhard Schölkopf. Parameter-efficient orthogonal finetuning via butterfly factorization. In *ICLR*, 2024.

Yinhan Liu, Myle Ott, Naman Goyal, Jingfei Du, Mandar Joshi, Danqi Chen, Omer Levy, Mike Lewis, Luke Zettlemoyer, and Veselin Stoyanov. Roberta: A robustly optimized bert pretraining approach, 2019.

Shashi Narayan, Shay B. Cohen, and Mirella Lapata. Don't give me the details, just the summary! topic-aware convolutional neural networks for extreme summarization. In *Proceedings of the 2018 Conference on Empirical Methods in Natural Language Processing*. Association for Computational Linguistics, 2018. doi: 10.18653/v1/d18-1206. URL http://dx.doi.org/10.18653/v1/D18-1206.

Vivek Ramanujan, Mitchell Wortsman, Aniruddha Kembhavi, Ali Farhadi, and Mohammad Rastegari. What's hidden in a randomly weighted neural network? In *2020 IEEE/CVF Conference on Computer Vision and Pattern Recognition (CVPR)*. IEEE, June 2020. doi: 10.1109/cvpr42600.2020.01191. URL http://dx.doi.org/10.1109/CVPR42600.2020.01191.

JO Ramsay, Jos ten Berge, and GPH Styan. Matrix correlation. *Psychometrika*, 49(3):403–423, 1984.

Nitish Srivastava, Geoffrey Hinton, Alex Krizhevsky, Ilya Sutskever, and Ruslan Salakhutdinov. Dropout: a simple way to prevent neural networks from overfitting. *The journal of machine learning research*, 15(1):1929–1958, 2014.

Hugo Touvron, Louis Martin, Kevin Stone, Peter Albert, Amjad Almahairi, Yasmine Babaei, Nikolay Bashlykov, Soumya Batra, Prajjwal Bhargava, Shruti Bhosale, Dan Bikel, Lukas Blecher, Cristian Canton Ferrer, Moya Chen, Guillem Cucurull, David Esiobu, Jude Fernandes, Jeremy Fu, Wenyin Fu, Brian Fuller, Cynthia Gao, Vedanuj Goswami, Naman Goyal, Anthony Hartshorn, Saghar Hosseini, Rui Hou, Hakan Inan, Marcin Kardas, Viktor Kerkez, Madian Khabsa, Isabel Kloumann, Artem Korenev, Punit Singh Koura, Marie-Anne Lachaux, Thibaut Lavril, Jenya Lee, Diana Liskovich, Yinghai Lu, Yuning Mao, Xavier Martinet, Todor Mihaylov, Pushkar Mishra, Igor Molybog, Yixin Nie, Andrew Poulton, Jeremy Reizenstein, Rashi Rungta, Kalyan Saladi, Alan Schelten, Ruan Silva, Eric Michael Smith, Ranjan Subramanian, Xiaoqing Ellen Tan, Binh Tang, Ross Taylor, Adina Williams, Jian Xiang Kuan, Puxin Xu, Zheng Yan, Iliyan Zarov, Yuchen Zhang, Angela Fan, Melanie Kambadur, Sharan Narang, Aurelien Rodriguez, Robert Stojnic, Sergey Edunov, and Thomas Scialom. Llama 2: Open foundation and fine-tuned chat models, 2023.

Roman Vershynin. High-dimensional probability. *University of California, Irvine*, 2020.

Alex Wang, Amanpreet Singh, Julian Michael, Felix Hill, Omer Levy, and Samuel Bowman. Glue: A multi-task benchmark and analysis platform for natural language understanding. In *Proceedings of the 2018 EMNLP Workshop BlackboxNLP: Analyzing and Interpreting Neural Networks for NLP*. Association for Computational Linguistics, 2018. doi: 10.18653/v1/w18-5446. URL http://dx.doi.org/10.18653/v1/W18-5446.

Yizhong Wang, Hamish Ivison, Pradeep Dasigi, Jack Hessel, Tushar Khot, Khyathi Raghavi Chandu, David Wadden, Kelsey MacMillan, Noah A Smith, Iz Beltagy, et al. How far can camels go? exploring the state of instruction tuning on open resources. *arXiv preprint arXiv:2306.04751*, 2023.

Thomas Wolf, Lysandre Debut, Victor Sanh, Julien Chaumond, Clement Delangue, Anthony Moi, Pierric Cistac, Tim Rault, Rémi Louf, Morgan Funtowicz, et al. Huggingface's transformers: State-of-the-art natural language processing. *arXiv preprint arXiv:1910.03771*, 2019.

Aolin Xu and Maxim Raginsky. Information-theoretic analysis of generalization capability of learning algorithms. In I. Guyon, U. Von Luxburg, S. Bengio, H. Wallach, R. Fergus, S. Vishwanathan, and R. Garnett (eds.), *Advances in Neural Information Processing Systems*, volume 30. Curran Associates, Inc., 2017.

Prateek Yadav, Leshem Choshen, Colin Raffel, and Mohit Bansal. Compeft: Compression for communicating parameter efficient updates via sparsification and quantization. *arXiv preprint arXiv:2311.13171*, 2023.

Yuchen Zeng and Kangwook Lee. The expressive power of low-rank adaptation, 2023.

Longteng Zhang, Lin Zhang, Shaohuai Shi, Xiaowen Chu, and Bo Li. Lora-fa: Memory-efficient low-rank adaptation for large language models fine-tuning, 2023a.

Qingru Zhang, Minshuo Chen, Alexander Bukharin, Nikos Karampatziakis, Pengcheng He, Yu Cheng, Weizhu Chen, and Tuo Zhao. Adalora: Adaptive budget allocation for parameter-efficient fine-tuning, 2023b.

A Related Work

LoRA Hu et al. (2021) has inspired a vast array of improvements to the basic technique. For example, quantization can reduce memory usage during training (Gholami et al., 2021; Dettmers et al., 2023; Guo et al., 2024). Also, the number of trainable parameters can be further reduced by adaptively allocating the rank (Zhang et al., 2023b), pruning during training (Benedek & Wolf, 2024), or pruning and quantizing after training (Yadav et al., 2023).

To further reduce the number of trainable LoRA parameters, the idea of reusing (randomly generated) weights or projections (Frankle & Carbin, 2018; Ramanujan et al., 2020) suggests strategies from learning diagonal matrices rescaling randomly-drawn and frozen B, A matrices (VeRA) (Kopiczko et al., 2024), deriving B and A from the SVD decomposition of the pre-trained W_0 and optimizing for a smaller matrix in the resulting basis (SVDiff) (Han et al., 2023), learning a linear combination of fixed random matrices (NOLA) (Koohpayegani et al., 2023), or fine-tuning using orthogonal matrices (BOFT) (Liu et al., 2024). As echoed in our empirical results, previous methods observe that freezing A in conventional LoRA preserves performance (Zhang et al., 2023a). While nearly *all* recent studies treat the two matrices asymmetrically in their initialization or freezing schemes, there is a lack of formal investigation into this asymmetry in low-rank adaptation.

Even before LoRA, fine-tuning was shown to succeed despite low dimensionality (Aghajanyan et al., 2021). Zeng & Lee (2023) specifically investigate the expressive power of LoRA, focusing on linear networks and linear parts of networks. Their analysis does not consider aspects such as the particular distribution of fine-tuning target data, generalization, and the differing roles of various factors.

B Full Theoretical Analysis

In this section, we analyze the asymmetry in prediction tasks and its effect on generalization. We discuss a general case rather than a specific neural network architecture, considering rank r adaptation of any parameter matrix $W = W_0 + BA$ used multiplicatively on some input-dependent vector, i.e.,

$$\text{layerOutput} = \psi((W_0 + BA) \cdot \phi(\text{layerInput}), \dots) \tag{3}$$

for some differentiable functions ψ, ϕ. Here, ψ may take more arguments depending on layerInput, which may have their own low rank adapted parameter matrices. This generic form encompasses both feedforward and attention layers.

In this setting, A serves to extract r features from $\phi(\text{layerInput})$, which are then used by B to predict some desired output for future layers. We will argue that training B to predict the output is crucial for correct outputs, while using a random A is often sufficient, as B can be optimized to use whatever information is retained in the r-dimensional projection $A \cdot \phi(\text{layerInput})$.

B.1 A, B asymmetry in prediction tasks

If we wish to reduce the effort of training both A and B in (3), in principle either A could be frozen and B tuned or B frozen and A tuned. As shown in §C and elsewhere, these two options are not empirically equivalent: It is best to freeze A and tune B. In this section, we seek to understand the principle behind this asymmetry by theoretically analyzing the fine-tuning of a class of prediction models. We first build intuition with least-squares linear regression.

B.1.1 Multivariate linear least-squares

As a simple example analogous to a single network layer, we study d_{in}-to-d_{out} least-squares linear regression (in (3), set ϕ, ψ to be identity). Specifically, suppose there is an input $X \in \mathbb{R}^{d_{in}}$, an output $Y \in \mathbb{R}^{d_{out}}$, and a pre-trained linear model

$$y_{pre}(X) = W_0 X + b_0,$$

where $W_0 \in \mathbb{R}^{d_{out} \times d_{in}}$ and $b_0 \in \mathbb{R}^{d_{out}}$. With this model held constant, our goal is regressing (Y_{targ}, X_{targ}) pairs where Y_{targ} is given by:

$$Y_{targ} = W_{targ} X_{targ} + b_{targ}$$

with $W_{targ} = W_0 + \Delta$. Following LoRA, we model the target Δ using a low rank update to the pre-trained W_0, i.e. $W = W_0 + BA$:

$$\hat{y}(x) = (W_0 + BA)x + b,$$

where $B \in \mathbb{R}^{d_{out} \times r}$ and $A \in \mathbb{R}^{r \times d_{in}}$ for some r.

To find an A and B that best matches the output, we optimize the least squares loss on the difference between $\hat{y}$ and Y_{targ}:

$$\mathcal{L}(A, B) = \mathbb{E}_{(Y_{targ}, X_{targ})}[\|Y_{targ} - (W_0 + BA)X_{targ} - b\|_2^2]. \tag{4}$$

Below, we present lemmas on minimizing this loss while freezing either A or B. In both, for simplicity, we set $b = b_{targ}$ and $\mathbb{E}[X_{targ}] = 0$ and defer proofs to Appendix E.

Lemma B.1 (Freezing A yields regression on projected **features**). *Optimizing $\mathcal{L}(A, B)$ while fixing $A = Q$ with $QQ^\top = I_r$ yields*

$$B^* = \Delta\Sigma Q^\top (Q\Sigma Q^\top)^{-1},$$

where $\Sigma = \mathrm{Cov}[X_{targ}]$, with expected loss

$$\mathcal{L}(Q, B^*) = \ d_{out}\sigma^2 + \mathrm{Tr}[\Delta\Sigma\Delta^\top] - \mathrm{Tr}[Q\Sigma\Delta^\top\Delta\Sigma Q^\top (Q\Sigma Q^\top)^{-1}].$$

Lemma B.2 (Freezing B yields regression on projected **outputs**). *Optimizing $\mathcal{L}(A, B)$ while fixing $B = U$ with $U^\top U = I_r$ yields*

$$A^* = U^\top (W_{targ} - W_0),$$

with expected loss

$$\mathcal{L}(A^*, U) = d_{out}\sigma^2 + \mathrm{Tr}[\Delta\Sigma\Delta^\top] - \mathrm{Tr}[U^\top\Delta\Sigma\Delta^\top U],$$

where $\Sigma = \mathrm{Cov}[X_{targ}]$.

Comparing the lemmas above, A^* is simply the U projection of the targeted change in weight matrix $\Delta = W_{targ} - W_0$. Unlike B^*, the optimal choice of A^* does not consider the input data distribution captured by Σ.

Intuitively, if the goal of adaptation is to approximate some desired output, then projecting away the majority (since $r \ll d_{out}$) of the output is undesirable. In contrast, projecting away a portion of the input feature space will be less damaging, if the information X_{targ} contains about Y_{targ} is redundant (c.f., neuron dropout (Srivastava et al., 2014) in neural network training) or if the distribution of X_{targ} tends to be low-rank.

Consider the following extreme example. If $\Sigma = FF^\top$ is at most rank r, e.g. if $F \in d_{in} \times r$, then for each X there exists[1] an $N = F^\dagger X \in \mathbb{R}^r$ such that $X = FN$. Suppose you have tuned a pair A_*, B_*. For any orthonormal $Q \in \mathbb{R}^{r \times d_{in}}$ (e.g. one drawn at random), we can write

$$B_*A_*X = B_*A_*FN = (B_*A_*F(QF)^{-1})QX,$$

i.e. regardless of A_*, B_*, for any (random) Q, there is an exactly equivalent LoRA adaptation with $A = Q$ and $B = (B_*A_*F(QF)^{-1})$. In this setting, therefore, randomizing A (to Q) is equally expressive to tuning it (using A_*).

This intuition is also reflected in the typical LoRA initialization. When doing full LoRA (tuning both A, B), A usually is initialized to a random Gaussian matrix, and B is initialized to zero. This procedure—presumably empirically derived by Hu et al. (2021)—intuitively fits our analysis above, since random A yields good random predictive features, in contrast to using a random output prediction basis. Initializing B to zero then starts the optimization at a zero perturbation of the pretrained model.

We validate the above intuition with the following theorem:

Theorem B.3 (A, B output fit asymmetry). *Consider the settings of Lemmas B.1 and B.2, and suppose U, Q are sampled uniformly from their respective Stiefel manifolds. Then, $\mathcal{L}(A^*, U) \geq \mathcal{L}(Q, B^*)$ with high probability as $d/r \to \infty$.*

[1]Here $F^\dagger$ denotes pseudoinverse.

In other words, the least-squares prediction loss of only fine-tuning B is at least as good as only fine-tuning A.

Intuition on asymmetry gap. Theorem B.3 is built on the following inequality:

$$\mathrm{Tr}[\Sigma Q^\top (Q\Sigma Q^\top)^{-1} Q\Sigma\Delta^\top\Delta] \geq \mathrm{Tr}[(Q^\top Q)\Sigma Q^\top (Q\Sigma Q^\top)^{-1} Q\Sigma\Delta^\top\Delta].$$

Let us consider an example regime to build intuition on the size of this gap. Following intuition that freezing A is most successful when the information content of the input is redundant (c.f., Aghajanyan et al. (2021)), suppose the distribution of X is low rank, i.e., Σ is of rank r_X. We can then write $\Sigma = U_X S_X U_X^\top$, where $U_X \in \mathbb{R}^{d_{in}\times r_X}$ is orthogonal and $S_X \in \mathbb{R}^{r_X\times r_X}$ is diagonal with nonnegative real entries.

For intuition, set $r_X = r$ and $S_X = \sigma^2 I_r$. We then have

$$\Sigma Q^\top (Q\Sigma Q^\top)^{-1} Q\Sigma\Delta^\top\Delta = \sigma^2 U_X U_X^\top \Delta^\top\Delta,$$

which no longer depends on Q. The expectation of the key inequality gap in (**??**) then becomes

$$\begin{aligned}&\mathbb{E}_Q \mathrm{Tr}[\Sigma Q^\top (Q\Sigma Q^\top)^{-1} Q\Sigma\Delta^\top\Delta] - \mathbb{E}_Q \mathrm{Tr}[(Q^\top Q)\Sigma Q^\top (Q\Sigma Q^\top)^{-1} Q\Sigma\Delta^\top\Delta] \\ &= \mathbb{E}_Q \mathrm{Tr}[(I - Q^\top Q)\sigma^2 U_X U_X^\top \Delta^\top\Delta] \to \left(1 - \frac{r}{d}\right) \mathrm{Tr}[U_X U_X^\top \Delta^\top\Delta]\end{aligned}$$

as d becomes large. In other words, the performance advantage of tuning B over A is large when $d \gg r$, which is the typical regime in practice.

B.1.2 Nonlinear losses and multilayer models

Recalling (3) with an input transformation ϕ and output transformation ψ, consider losses on the output of the form

$$\mathcal{L}(W) = \sum_{i=1}^{n} h(f(\psi(W\phi(x_i)))) - y_i^\top f(\psi(W\phi(x_i))), \tag{5}$$

where f, h are differentiable functions specified by the desired loss, $y_i \in \mathbb{R}^K$, $x_i \in \mathbb{R}^{d_{in}}$, and $W \in \mathbb{R}^{d_{out}\times d_{in}}$. This class contains logistic regression (with y being a one-hot encoded class vector), least-squares regression, and generalized linear regression—including a neural network with cross entropy loss with one layer being tuned.

We next analyze the gradient of this loss. Our argument is stated with one adapted parameter matrix, but it directly applicable to multilayer and transformer networks with multiple matrices being adapted, where ϕ, ψ, and f will in that scenario vary depending on each parameter matrix's position in the network; ϕ, ψ, and f will depend on other parameter matrices and the current value of their adaptations (by definition of gradients). The interpretation will now be that fixing A when adapting a parameter matrix $W^{(\ell)}$ projects the inputs of the corresponding parameter matrix to a lower-dimensional subspace while retaining the ability to fully match the outputs, and fixing B correspondingly projects the parameter matrix's outputs.

For simplicity of notation, the remaining derivation in this section takes ϕ, ψ to be the identity; the extension to general ϕ, ψ is clear. Then, the gradient of (5) is

$$\nabla_W \mathcal{L}(W) = \sum_{i=1}^{n} J_f^\top (Wx_i) \left[\nabla h(f(Wx_i)) - y_i\right] x_i^\top, \tag{6}$$

where J_f is the Jacobian of f. Starting from this formula, below we incorporate (3) by taking $W = W_0 + BA$.

Freezing A. Freezing $A = Q$ yields

$$\nabla_B \mathcal{L}(BQ + W_0) = \sum_{i=1}^{n} J_f^\top((BQ + W_0)x_i) \left[\nabla h(f((W_0 + BQ)x_i)) - y_i\right] (Qx_i)^\top.$$

Like the least-squares case, the input data is projected by Q but the output y_i is unaffected.

Freezing B. Freezing $B = U$ yields

$$\nabla_A \mathcal{L}(UA + W_0) = U^\top \sum_{i=1}^{n} J_f^\top ((UA + W_0)x_i) \left[\nabla h(f((W_0 + UA)x_i)) - y_i\right] x_i^\top.$$

Here, the coefficient of $x_i^\top$ can be thought of as the output fit term. It includes the Jacobian of f since f is applied between the weights and the output. Compared to (6) and (**??**), in (**??**) this output fit term is projected by U. If f is (near) linear, then this projection will be (approximately) data-independent, highlighting the loss of output information when freezing B.

Hence, in this more general setting, the different roles of A and B are still apparent, and we expect an asymmetry in being able to fit the output.

Example: Logistic regression. For multiclass logistic regression, we have a training dataset $\{(x_i, c_i)\}_{i=1}^n$ where $x_i \in \mathbb{R}^d$ (features) and $c_i \in \{1, \dots, K\}$ (label). Denote by $y_i \in \mathbb{R}^K$ the vector with $y_{c_i} = 1$ and $y_k = 0$ for $k \neq c_i$. The log likelihood is the cross-entropy error

$$\mathcal{L}(w_1, \dots, w_K) = \sum_{i=1}^{n} \sum_{k=1}^{K} y_i \ln(p_{i,k}), \tag{7}$$

where $p_{i,k} = \frac{\exp(w_k^\top x_i)}{\sum_{l=1}^K \exp(w_l^\top x_i)}$ and $w_k \in \mathbb{R}^d$. Let $W \in \mathbb{R}^{K \times d}$ whose k-th row is w_k. Then, (7) becomes

$$\mathcal{L}(W) = \sum_{i=1}^{n} \ln(\mathbf{1}^\top e^{W x_i}) - y_i^\top W x_i,$$

where $\mathbf{1}$ is the column vector of size K with all elements equal to 1; note $y_i^\top \mathbf{1} = 1$ due to the one-hot structure. This loss can be put in the form (5) by setting $f(z) = z$ and $h(z) = \ln(\mathbf{1}^\top e^z)$. For freezing, we then have

$$\nabla_A \mathcal{L}(UA) = U^\top \sum_{i=1}^{n} (y_i - p_i(UA)) x_i^\top \qquad \text{and} \nabla_B \mathcal{L}(BQ) = \sum_{i=1}^{n} (y_i - p_i(BQ))(Qx_i)^\top,$$

where $p_i(W) = \frac{e^{W x_i}}{\mathbf{1}^\top e^{W x_i}} \in \mathbb{R}^K$. Freezing $B = U$, as in least-squares, implies that each output y_i is projected as $U^\top y_i$, implying that, at best, the model can hope to only learn outputs in the small random subspace U. In contrast, freezing $A = Q$ is equivalent to logistic regression on the full output with features projected by Q: $\{(Qx_i, y_i)\}_{i=1}^n$.

B.2 Advantages of tuning only B over BA together

In the previous section, we established that fine-tuning B alone is typically superior to fine-tuning A alone. It remains, however, to motivate fine-tuning B alone over fine-tuning both A and B together. In this section, we show that the reduced amount of adapted parameters by (roughly) half provides computational gains and improvements in information-theoretic generalization bounds.

B.2.1 Number of parameters

The key benefit of LoRA is parameter efficiency, which saves memory during training, storage and communication Lialin et al. (2023). Fine-tuning B alone as opposed to both A and B reduces the number of parameters by a factor of $\frac{d_{out}}{d_{out}+d_{in}}$, which equals 0.5 when $d_{in} = d_{out}$.

B.2.2 Generalization bounds

Consider a learning task, where the training examples lie in $\mathcal{Z} = \mathcal{X} \times \mathcal{Y}$; here, $\mathcal{X}$ denotes the feature space and $\mathcal{Y}$ is the label space. Suppose one observes a training set $S_n \triangleq (Z_1, \dots, Z_n) \in \mathcal{Z}^n$, with n i.i.d. training examples from unknown distribution μ. Denote by $\mu^{\otimes n} = \mu \times \cdots \times \mu$ the distribution of S_n. The objective of the learner is to find a predictor $f : \mathcal{X} \to \mathcal{Y}$ that maps features to their labels. We assume each predictor is parameterized by $w \in \mathcal{W}$ (e.g., if f is a neural network, w denotes its weights). Denote by $\mathcal{A} : \mathcal{Z}^n \to \mathcal{W}$ the learning algorithm which selects a predictor given S_n. $\mathcal{A}$ is,

in general, a probabilistic mapping, and we denote by $P_{W|S_n}$ the distribution of its output W given input S_n. If $\ell : \mathcal{W} \times \mathcal{Z} \to \mathbb{R}_+$ is a loss, we define:

$$\text{Population risk:} \quad \mathcal{R}_\mu(w) \triangleq \mathbb{E}_{Z\sim\mu}[\ell(w, Z)]$$
$$\text{Empirical risk:} \quad \widehat{\mathcal{R}}_n(w) \triangleq \frac{1}{n}\sum_{i=1}^{n} \ell(w, Z_i).$$

The generalization error of $\mathcal{A}$ is

$$\text{gen}(\mu, \mathcal{A}) \triangleq \mathbb{E}_{(W,S_n)\sim P_{W|S_n}\times\mu^{\otimes n}}[\mathcal{R}_\mu(W) - \widehat{\mathcal{R}}_n(W)]\,.$$

We bound this generalization error using the information-theoretic generalization framework of Xu & Raginsky (2017). Consider the following incarnations of fine-tuning algorithms, corresponding to classic LoRA (tuning both A, B matrices), tuning only B, and tuning only A:

Definition B.4 (Fine-tuning algorithms)**.** Let $\mathbf{W} = \{W_i\}_{i=1}^L$ be the L parameter matrices of a pretrained model. Let $\mathcal{I} \subseteq \{1, \ldots, L\}$ be a specified subset of the parameter matrices to be fine-tuned. Given a fine-tuning training set S_n, let r be a chosen rank and suppose each tuned parameter is quantized to q bits. We define the following algorithmic frameworks (other details can be arbitrary) for choosing an adaptation $\mathbf{\Delta W} = \{\Delta_i\}_{i\in\mathcal{I}}$, yielding a fine-tuned $W_{tuned} = \{W_{tuned,i}\}_{i=1}^L$ with $W_{tuned,i} = W_i + \Delta_i$ for $i \in \mathcal{I}$ and $W_{tuned,i} = W_i$ otherwise:

- $\mathcal{A}_{BA}$: For each $i \in \mathcal{I}$, constrain $\Delta_i = B_i A_i$ and optimize $\{B_i, A_i\}_{i\in\mathcal{I}}$ to fit the data S_n.
- $\mathcal{A}_B$: For each $i \in \mathcal{I}$, sample $Q_i \in \mathbb{R}^{r\times d_{in}^{(i)}}$ at random, constrain $\Delta_i = B_i Q_i$, and optimize $\{B_i\}_{i\in\mathcal{I}}$ to fit the data S_n.
- $\mathcal{A}_A$: For each $i \in \mathcal{I}$, sample $U_i \in \mathbb{R}^{d_{out}^{(i)}\times r}$ at random, constrain $\Delta_i = U_i A_i$, and optimize $\{A_i\}_{i\in\mathcal{I}}$ to fit the data S_n.

We have the following lemma, proved in Appendix F:

Lemma B.5 (Generalization bounds on adapting A and/or B)**.** *Consider the algorithms of Definition B.4. Assume that $\ell^{\mathbf{W},\mathbf{b}}(\Delta\mathbf{W}, \widetilde{Z})$ is σ-sub-Gaussian[2] under $(\Delta\mathbf{W}, \widetilde{Z}) \sim P_{\Delta\mathbf{W}|\mathbf{W},\mathbf{b}} \times \mu$. Then,*

$$|\text{gen}(\mu, \mathcal{A}_{BA})| \le \sqrt{\frac{2rq\sigma^2 \ln 2}{n}\sum_{i\in\mathcal{I}}(d_{in}^{(i)} + d_{out}^{(i)})},$$
$$|\text{gen}(\mu, \mathcal{A}_{B})| \le \sqrt{\frac{2rq\sigma^2 \ln 2}{n}\sum_{i\in\mathcal{I}} d_{out}^{(i)}},$$
$$|\text{gen}(\mu, \mathcal{A}_{A})| \le \sqrt{\frac{2rq\sigma^2 \ln 2}{n}\sum_{i\in\mathcal{I}} d_{in}^{(i)}}.$$

This generalization bound increases with the number of parameters being tuned, which is an increasing function of r and the dimensions of the parameter matrices. Importantly, since tuning just one factor (A or B) involves tuning fewer parameters than A and B together, the generalization bound is correspondingly smaller. In the case where the $d_{in}^{(i)} = d_{out}^{(i)}$, the bound for tuning one factor only is a factor of $\sqrt{2}$ smaller than the bound for tuning both factors, implying that the rank r for $\mathcal{A}_B$ could be doubled and have a generalization bound matching that of $\mathcal{A}_{BA}$.

B.3 Discussion of theoretical analysis

The previous two sections establish two conclusions: (1) Tuning A has limited importance when trying to match a desired output; and (2) Tuning one factor instead of two reduces the number of parameters for the same r, while improving generalization bounds and potentially providing memory benefits.

Given a fixed parameter count and generalization budget, therefore, we can use a larger $r = r_B$ when fine-tuning B alone than the r_{BA} that would be used on standard LoRA fine-tuning both A and B.

[2]Bounded losses are sub-Gaussian.

Table 4: Different adaptation methods on the GLUE benchmark. We report the overall (matched and mismatched) accuracy for MNLI, Matthew's correlation coefficient for CoLA, Pearson correlation for STS-B, and accuracy for other tasks. Higher is better for all metrics.

Model & Method	# Trainable Parameters	MNLI	SST-2	MRPC	CoLA	QNLI	RTE	STS-B	Avg.
LoRA ($r = 8$)	0.8%	$90.3_{\pm.07}$	$95.6_{\pm0.36}$	$90.3_{\pm0.85}$	$64.4_{\pm1.8}$	$94.0_{\pm0.29}$	$84.1_{\pm0.96}$	$91.5_{\pm0.16}$	87.2
AdaLoRA	2.5%	$90.4_{\pm.37}$	$95.9_{\pm.13}$	$90.1_{\pm.54}$	$67.5_{\pm1.3}$	$94.7_{\pm.22}$	$85.4_{\pm.20}$	$91.3_{\pm1.0}$	87.9
$(IA)^3$	0.7%	$90.0_{\pm.21}$	$95.4_{\pm.17}$	$83.7_{\pm.13}$	$57.6_{\pm.67}$	$93.7_{\pm.07}$	$70.3_{\pm1.5}$	$87.0_{\pm0.4}$	82.5
LoRA-FA	0.3%	$90.3_{\pm.06}$	$95.6_{\pm.17}$	$90.6_{\pm.32}$	$67.3_{\pm2.3}$	$93.4_{\pm.61}$	$82.4_{\pm1.4}$	$91.2_{\pm.29}$	87.3
$\hat{\mathbf{B}}_0 A_{rand}$ ($r = 8$)	0.3%	$90.1_{\pm.19}$	$\underline{95.8}_{\pm.29}$	$89.7_{\pm.13}$	$\mathbf{\underline{67.5}}_{\pm\mathbf{1.2}}$	$\underline{94.0}_{\pm.27}$	$82.8_{\pm1.5}$	$\mathbf{\underline{91.9}}_{\pm\mathbf{.26}}$	87.4
$\hat{\mathbf{B}}_0 A_{rand}$ ($r = 16$)	0.8%	$90.1_{\pm.20}$	$\mathbf{\underline{96.1}}_{\pm\mathbf{.18}}$	$\mathbf{\underline{90.7}}_{\pm\mathbf{.90}}$	$66.1_{\pm2.6}$	$\mathbf{\underline{94.4}}_{\pm\mathbf{.10}}$	$\mathbf{\underline{84.1}}_{\pm\mathbf{.96}}$	$91.2_{\pm.42}$	87.5
$B_{rand}\hat{\mathbf{A}}_0$ ($r = 8$)	0.3%	$\mathbf{\underline{90.3}}_{\pm\mathbf{.18}}$	$95.5_{\pm.66}$	$89.3_{\pm.09}$	$58.7_{\pm2.5}$	$93.8_{\pm.21}$	$77.1_{\pm1.3}$	$90.7_{\pm.31}$	84.2
$B_{rand}\hat{\mathbf{A}}_0$ ($r = 16$)	0.8%	$89.9_{\pm.19}$	$\underline{95.6}_{\pm.64}$	$90.2_{\pm0.23}$	$60.3_{\pm3.3}$	$93.9_{\pm0.25}$	$80.4_{\pm0.21}$	$90.9_{\pm0.13}$	85.9

This addition provides more expressive power for the same number of parameters without loss of generalization bounds. Hence, when matching parameter or generalization budget, we expect that fine-tuning a rank-r_B B typically improves performance over fine-tuning a rank-r_{BA} BA LoRA adaptation.

C Experiments

We investigate the asymmetry of low-rank adaptation methods with RoBERTa (Liu et al., 2019), BART (Lewis et al., 2020), Llama-2 (Touvron et al., 2023), and Vistion Transformer (Dosovitskiy et al., 2020). We evaluate the performance of fine-turning strategies on natural language understanding (GLUE (Wang et al., 2018), MMLU (Hendrycks et al., 2020)), natural language generation (XSum (Narayan et al., 2018) and CNN/DailyMail (Chen et al., 2016)), and multi-domain image classification (Gulrajani & Lopez-Paz, 2020).

We implement all algorithms using PyTorch starting from the publicly-available Huggingface Transformers code base (Wolf et al., 2019). The conventional LoRA method applies a scaling coefficient α/r to ΔW. Following LoRA (Hu et al., 2021), we fix $\alpha = 2r$ to be twice the rank. Throughout our experiments, we use $\hat{A}$ to indicate matrix A is being updated during fine-tuning and use subscripts $\{$*rand,* 0*, km*$\}$ to indicate that the matrix is initialized as a random orthonormal matrix, zero matrix, and the random uniform initialization used in the original LoRA, respectively. Note that a properly normalized $d \times r$ random matrix with independent entries will have close to orthonormal columns when $d \gg r$ (see e.g. Theorem 4.6.1 of Vershynin (2020)), implying that the random orthonormal and random uniform initializations should be essentially equivalent.

We compare to the following methods:

1. **Full fine-tuning (FT):** The most straightforward adaptation method, which initializes model parameters with the pre-trained weights and updates the whole model with gradient back-propagation.
2. **Linear Probing (LP) (Kumar et al., 2022):** A simple yet effective method that updates the last linear layer.
3. **IA^3 (Liu et al., 2022):** Injects learned vectors in the attention and feedforward modules.
4. **LoRA:** (Hu et al., 2021) Fine-tunes both A and B matrices of an additive BA adaptation as introduced in previous sections, with a separate adaptation for each query/key/value parameter matrix.
5. **AdaLora:** (Zhang et al., 2023b) A variant of LoRA that adaptively changes the rank for each layer.

C.1 Natural Language Understanding

We use the General Language Understanding Evaluation (GLUE, Wang et al., 2018) to evaluate the fine-tuning performance of different fine-tuning strategies. The GLUE benchmark contains a wide variety of tasks including question-answering, textual similarity, and sentiment analysis. We applied

Table 5: Different initialization of classic LoRA, setting either A or B to be zeros. Note that the trained result is not sensitive to different initializations, with performance differences tending to be smaller than the standard error.

Model & Method	# Trainable Parameters	MNLI	SST-2	MRPC	CoLA	QNLI	RTE	STS-B	Avg.
$\hat{\mathbf{B}}_0\hat{\mathbf{A}}_V$	0.8%	**90.4**$_{\pm 0.11}$	95.9$_{\pm 0.16}$	90.7$_{\pm 0.84}$	64.0$_{\pm 0.50}$	94.4$_{\pm 0.16}$	84.1$_{\pm 0.15}$	91.8$_{\pm 00.15}$	87.3
$\hat{\mathbf{B}}_0\hat{\mathbf{A}}_{rand}$	0.8%	**90.4**$_{\pm 0.15}$	96.0$_{\pm 0.11}$	91.5$_{\pm 1.1}$	64.1$_{\pm 0.67}$	94.5$_{\pm 0.11}$	**85.6**$_{\pm 0.96}$	**92.0**$_{\pm 0.31}$	87.7
$\hat{\mathbf{B}}_U\hat{\mathbf{A}}_0$	0.8%	90.3$_{\pm 0.07}$	**96.1**$_{\pm .18}$	**91.7**$_{\pm 0.33}$	64.9$_{\pm 1.5}$	**94.7**$_{\pm 0.33}$	84.8$_{\pm 0.96}$	91.9$_{\pm 0.19}$	87.8
$\hat{\mathbf{B}}_{rand}\hat{\mathbf{A}}_0$	0.8%	90.3$_{\pm 0.27}$	96.0$_{\pm .26}$	90.8$_{\pm 0.51}$	**66.0**$_{\pm 1.01}$	94.5$_{\pm 0.38}$	83.6$_{\pm 1.5}$	**92.0**$_{\pm 0.18}$	87.8

Table 6: R-1/2/L (%) on text summarization with BART-large on XSum and CNN/DailyMail.

Method	# Param.	XSum	CNN/DailyMail
$\hat{\mathbf{B}}_0 A_{rand,r=16}$	0.44 %	**42.91 / 19.61 / 34.64**	**43.65 / 20.62 / 40.72**
$B_{rand}\hat{\mathbf{A}}_{0,r=16}$	0.44 %	42.37 / 19.30 / 34.29	43.38 / 20.36 / 40.48
$\hat{\mathbf{B}}_0\hat{\mathbf{A}}_{rand,r=8}$	0.44 %	43.78 / **20.47 / 35.53**	43.96 / 20.94 / 41.00
$\hat{\mathbf{B}}_{rand}\hat{\mathbf{A}}_{0,r=8}$	0.44 %	**43.80** / 20.39 / 35.48	**44.07 / 21.08 / 41.19**

Table 7: DomainBed results (mean accuracy and standard deviation in %). ID and OOD denote in-domain and out-of-domain test error, respectively. For OOD we report the average performance across different environments.

Method	# Param.	VLCS		PACS		OfficeHome	
		(ID)	(OOD)	(ID)	(OOD)	(ID)	(OOD)
LoRA $_{r=8}$	0.46%	73.51$_{\pm 0.62}$	56.43$_{\pm 1.96}$	94.94$_{\pm 0.56}$	**75.58**$_{\pm 0.92}$	78.54$_{\pm 1.49}$	74.46$_{\pm 0.40}$
LP	0.00%	75.58$_{\pm 1.66}$	71.70$_{\pm 1.04}$	81.62$_{\pm 0.34}$	61.73$_{\pm 1.25}$	58.38$_{\pm 0.76}$	68.59$_{\pm 0.22}$
Full Fine-tuning	100%	76.21$_{\pm 1.95}$	64.87$_{\pm 6.44}$	**98.15**$_{\pm 0.56}$	74.90$_{\pm 2.43}$	**80.67**$_{\pm 1.22}$	63.23$_{\pm 0.64}$
$\hat{\mathbf{B}}A_{rand,r=8}$	0.29%	77.40$_{\pm 2.30}$	**75.81**$_{\pm 1.65}$	92.45$_{\pm 2.68}$	72.55$_{\pm 1.03}$	77.66$_{\pm 0.89}$	77.72$_{\pm 0.32}$
$\hat{\mathbf{B}}A_{rand,r=16}$	0.46%	**79.10**$_{\pm 1.41}$	75.40$_{\pm 1.24}$	93.52$_{\pm 0.20}$	73.76$_{\pm 0.67}$	77.63$_{\pm 0.84}$	**77.85**$_{\pm 0.33}$
$B_{rand}\hat{\mathbf{A}}_{r=8}$	0.29%	76.71$_{\pm 0.93}$	72.50$_{\pm 0.89}$	92.02$_{\pm 1.07}$	66.25$_{\pm 0.80}$	72.36$_{\pm 0.69}$	73.66$_{\pm 0.35}$

fine-tuning methods to the RoBERTa (large) model (Liu et al., 2019), which has 355M parameters. To enable a fair comparison, we initialize the weights for all tasks with the original pretrained RoBERTa weights.

In Table 4 (see the appendix for an expanded table), we compare different freezing & initialization strategies with LoRA and other baselines. We underline to indicate that performance is better than conventional LoRA also we use **bold** to denote the best performance when freezing one of the matrices. First, we can see a clear trend where solely updating the B matrix outperforms just learning the A matrix. In addition, when doubling the rank to match the trainable parameters, $\hat{\mathbf{B}}_0 A_{orth}$ consistently outperforms conventional LoRA. This confirms our hypothesis in §B.3 that any loss in expressive power by not tuning A can be made up for by the larger intrinsic rank of B at no additional parameter cost. In fact, its performance statistically matches that of AdaLoRA, which uses over 3 times the parameters (incurring the associated memory and training costs).

To assess the effects of different initialization methods for low-rank adaptation, we investigate different initialization methods thoroughly in Table 5. We can see that the best results always come from orthogonal initialization, which further supports our conclusions in §B.

C.2 Natural Language Generation

To investigate the asymmetry of low-rank fine-tuning in natural language generation (NLG), we fine-tune a BART-large model (Lewis et al., 2020) and evaluate model performance on the XSum (Narayan et al., 2018) and CNN/DailyMail (Chen et al., 2016) datasets. Following Zhang et al. (2023b), we apply low-rank adaptation to every query/key/value matrix and report ROUGE 1/2/L scores (R-

Table 8: Accuracy (%) on MMLU benchmark.

Method	# Param.	0-shot				
		Hums	STEM	Social	Other	Avg
Llama-2-7B	100%	34.22	29.58	34.64	35.60	34.93
LoRA $_{r=32}$	0.24%	40.12	33.92	43.21	**45.21**	40.56
$\hat{\mathbf{B}}_0 A_{rand,r=32}$	0.12%	**44.17**	**36.00**	**46.88**	45.14	**43.01**
$B_{rand}\hat{\mathbf{A}}_{0,r=32}$	0.12%	35.72	31.13	42.05	41.24	37.75

1/2/L, (Lin, 2004)). We fine-tune models for 15 epochs. We select the beam length as 8 and batch size as 48 for XSum, and the beam length as 4, batch size as 48 for CNN/DailyMail. More details of the configurations are in the Appendix G.

The results are summarized in Table 6. In the first two rows, we observe the asymmetry between the factors since freezing A and only updating B always outperforms only updating A. The last two rows show the results of tuning both matrices with different initializations, showing that the asymmetry is not explained by the initialization strategy.

C.3 Massive Multitask Language Understanding

We fine-tune the pretrained Llama-2-7B model (Touvron et al., 2023) using instruction tuning on the Alpaca dataset (Wang et al., 2023). We assess the asymmetry on the MMLU benchmark (Hendrycks et al., 2020), which consists of 57 distinct language tasks. As shown in Table 8, the asymmetry also exists in larger language models, and updating B consistently outperforms updating A. Moreover, it also outperforms standard LoRA except for "Other" where it matches the performance, reflecting the benefits of being able to increase r without tuning more parameters.

C.4 Vision Transformers and Generalization

We next measure generalization, motivated by the theory in §B.2. In particular, we work with ViTs in image classification tasks using the Domainbed testbed for domain generalization Gulrajani & Lopez-Paz (2020). Domainbed contains several datasets, each composed of multiple environments (or domains). Classes in each environment tend to be similar at a high level but differ in terms of style. We fine-tune a pre-trained ViT, originally trained on ImageNet, on the LabelMe, Cartoon, and Clipart environments within the VLCS, PACS, and Office-Home datasets, respectively. We employ different benchmark fine-tuning methods such as full fine-tuning, linear probing, and LoRA, and compare their performance to freezing either A or B in in-domain and out-of-domain generalization. We adhere to the original 80% training and 20% testing splits.

Results are presented in Table 7. In line with our expectations, randomly initializing and freezing matrix A while only updating matrix B generally results in better out-of-domain test accuracy. We report additional generalization results in Appendix I, in which we compare the train set and test set accuracy of the different approaches. We consistently find that fine-tuning a single matrix leads to smaller gaps between these two quantities compared to LoRA, paralleling the corresponding reduction in the generalization bounds of §B.2.

D Similarity metric in Figure 1

To measure the similarity of learned A and B matrices we adopted a measure that accounts for the invariance of LoRA fine-tuning. Let $\Delta W = BA$ denote the learned LoRA adapter. Since $BA = BCC^{-1}A$ for any invertible matrix $C \in \mathbb{R}^{r\times r}$, we can define $\tilde{B} = BC$ and $\tilde{A} = C^{-1}A$ resulting in the same LoRA adapter $\Delta W = \tilde{B}\tilde{A}$. Thus, to measure the similarity of LoRA matrices we need a metric that is invariant to invertible linear transformations, i.e., dissimilarity$(B, BC) = 0$ for any invertible C. In our experiment, we used Canonical Correlation Analysis goodness of fit (Ramsay et al., 1984), similar to prior work comparing neural network representations (Kornblith

et al., 2019). The key idea is to compare orthonormal bases of the matrices, thus making this similarity metric invariant to invertible linear transformations.

More specifically, given two matrices $X \in \mathbb{R}^{n \times r_1}$ and $Y \in \mathbb{R}^{n \times r_2}$, the similarity is computed as $\|U_Y^\top U_X\|_F^2 / \min\{r_1, r_2\}$, where U_X / U_Y is the orthonormal bases for the columns of X/Y. Following a similar method as in Hu et al. (2021), for A we perform SVD and use the right-singular unitary matrices as the bases, and use left-singular unitary matrices for B.

E ASYMMETRY PROOFS FOR MULTIVARIATE LEAST SQUARES

E.1 PROOF OF LEMMA B.2

Consider freezing $B = U$ where U is orthogonal ($U^\top U = I_r$) and fine-tuning A. The objective becomes

$$\begin{aligned}
A^* &= \arg\min_A \mathcal{L}(A, U) \\
&= \arg\min_A \mathbb{E}_{(Y_{targ}, X_{targ})} \|Y_{targ} - (W_0 + UA)X_{targ} - b\|_2^2 \\
&= \arg\min_A \mathbb{E} \|(W_{targ}X_{targ} - W_0 X_{targ}) - UAX_{targ}\|_2^2 \\
&= \arg\min_A \mathbb{E} \left\|U^\top((W_{targ} - W_0)X_{targ} + n) - AX_{targ}\right\|_2^2 \\
&= U^\top \Delta.
\end{aligned}$$

Interestingly, note that this solution A^* does not depend on the distribution of X_{targ}, it is simply the projection of the difference between the pretrained W_0 and the target W_{targ}. This is because, intuitively, freezing B is projecting down the *outputs* into r dimensional space, and then optimizing A to match these projected outputs. It can be shown that the expected squared prediction error is

$$\mathcal{L}(A^*, U) = d_{out}\sigma^2 + \mathrm{Tr}[\Delta\Sigma\Delta^\top] - \mathrm{Tr}[U^\top\Delta\Sigma\Delta^\top U],$$

where $\Sigma = \mathrm{Cov}[X_{targ}]$.

E.2 PROOF OF LEMMA B.1

Consider freezing $A = Q$ where Q is orthogonal ($QQ^\top = I_r$) and fine-tuning B. The objective becomes

$$\begin{aligned}
&B^* \\
&= \arg\min_B \mathcal{L}(Q, B) \\
&= \arg\min_B \mathbb{E}_{(Y_{targ}, X_{targ})} \|Y_{targ} - (W_0 + BQ)X_{targ}\|_2^2 \\
&= \arg\min_B \mathbb{E} \|(Y_{targ} - W_0 X_{targ}) - B(QX_{targ})\|_2^2,
\end{aligned}$$

which is simply an ordinary least squares regression problem mapping QX_{targ} to $(Y_{targ} - W_0 X_{targ})$. The solution is known to be

$$B^* = \Delta\Sigma Q^\top (Q\Sigma Q^\top)^{-1}$$

yielding an expected squared prediction error of

$$\begin{aligned}
\mathcal{L}(Q, B^*) = d_{out}\sigma^2 &+ \mathrm{Tr}[\Delta\Sigma\Delta^\top] \\
&- \mathrm{Tr}[Q\Sigma\Delta^\top\Delta\Sigma Q^\top (Q\Sigma Q^\top)^{-1}].
\end{aligned}$$

Note that the solution is now clearly dependent on the distribution of X_{targ}, and the first two terms of the squared prediction error are the same but the third term is different.

E.3 Proof of Theorem B.3

The third term in the expression for freezing A is

$$\begin{aligned} III_A =& \mathrm{Tr}[Q\Sigma\Delta^\top\Delta\Sigma Q^\top(Q\Sigma Q^\top)^{-1}] \\ &\geq \mathrm{Tr}[Q\Sigma\Delta^\top\Delta Q^\top Q\Sigma Q^\top(Q\Sigma Q^\top)^{-1}] \\ &= \mathrm{Tr}[Q\Sigma\Delta^\top\Delta Q^\top], \end{aligned}$$

where the inequality follows by Von Neumann's trace inequality and the fact that the product of two positive semidefinite matrices has nonnegative real eigenvalues. Compare to the third term in the expression for freezing B:

$$III_B = \mathrm{Tr}[U^\top\Delta\Sigma\Delta^\top U].$$

Recall that U, Q are drawn uniformly at random from their respective Stiefel manifolds. Then

$$\mathbb{E}[III_B] \to \frac{r}{d}\mathrm{Tr}[\Delta\Sigma\Delta^\top]$$

and we have

$$\begin{aligned} &\mathbb{E}[III_A] \geq \mathbb{E}[\mathrm{Tr}[Q\Sigma\Delta^\top\Delta Q^\top]] \\ &\to \frac{r}{d}\mathrm{Tr}[\Sigma\Delta^\top\Delta] = \frac{r}{d}\mathrm{Tr}[\Delta\Sigma\Delta^\top] \to \mathbb{E}[III_B]. \end{aligned}$$

Hence $\lim_{d/r\to\infty}\mathbb{E}[III_A] \geq \lim_{d/r\to\infty}\mathbb{E}[III_B]$, implying that freezing A to a random orthogonal matrix achieves lower mean squared error loss than freezing B.

F Proof of Lemma B.5: Generalization bounds

We use the following bound on the generalization error is from Xu & Raginsky (2017), specialized to our setting and notation.

Theorem F.1 (specialized from Xu & Raginsky (2017))**.** *Denote by $\mathcal{A}$ a LoRA-based fine-tuning algorithm, which outputs $\Delta\mathbf{W}$ given S_n. Assume that $\ell^{\mathbf{W},\mathbf{b}}(\Delta\mathbf{W}, \widetilde{Z})$ is σ-sub-Gaussian under $(\Delta\mathbf{W}, \widetilde{Z}) \sim P_{\Delta\mathbf{W}|\mathbf{W},\mathbf{b}} \times \mu$. Then,*

$$|\mathrm{gen}(\mu, \mathcal{A})| \leq \sqrt{\frac{2\sigma^2}{n}\mathsf{I}\Delta\mathbf{W}; S_n|\mathcal{A}, \mathbf{W}}. \tag{8}$$

We consider the case of tuning B only first. Applying the above theorem, note that here

$$\begin{aligned} \mathsf{I}\Delta\mathbf{W}; S_n|\mathcal{A}_B, \mathbf{W} &= \mathsf{I}\{B_iQ_i\}_{i\in\mathcal{I}}; S_n|\mathcal{A}_B, \mathbf{W} \\ &= \mathsf{I}\{B_i\}_{i\in\mathcal{I}}; S_n|\mathcal{A}_B, \mathbf{W}, \end{aligned}$$

where we have used standard information-theoretic equalities, noted that the Q_i are here considered fixed constants as they are not trained.

We can now bound this expression as

$$\begin{aligned} \mathsf{I}\{B_i\}_{i\in\mathcal{I}}; S_n|\mathcal{A}_B, \mathbf{W} &\leq H(\{B_i\}_{i\in\mathcal{I}}) \\ &\leq qr\sum_{i\in\mathcal{I}} d_{out}^{(i)}, \end{aligned}$$

where we have noted that mutual information is upper bounded by discrete entropy, and entropy in turn is upper bounded by the uniform distribution over its possible support set. The bounds for the other two algorithms are similar.

G Text Generation Training Details

The configuration of our experiments on text generation is listed in Table 9.

Table 9: Hyper-parameter setup for summarization tasks.

Dataset	learning rate	batch size	# epochs	γ	t_i	Δ_T	t_f
XSum	5×10^{-4}	48	25	0.1	6000	100	50000
CNN/DailyMail	5×10^{-4}	48	15	0.1	5000	100	85000

Table 10: Different adaptation methods on the GLUE benchmark. We report the overall (matched and mismatched) accuracy for MNLI, Matthew's correlation coefficient for CoLA, Pearson correlation for STS-B, and accuracy for other tasks. Higher is better for all metrics.

Model & Method	# Trainable Parameters	MNLI	SST-2	MRPC	CoLA	QNLI	RTE	STS-B	Avg.
Full FT	355.0M								
LoRA ($r = 8$)	0.8M	$90.3_{\pm.07}$	$95.6_{\pm0.36}$	$90.3_{\pm0.85}$	$64.4_{\pm1.8}$	$94.0_{\pm0.29}$	$84.1_{\pm0.96}$	$91.5_{\pm0.16}$	
AdaLoRA	?M								
$(IA)^3$	?M								
$\hat{B}_0 A_V$ ($r = 8$)	0.3M	$90.1_{\pm.09}$	$95.5_{\pm.01}$	$90.8_{\pm.24}$	$63.8_{\pm4.2}$	$94.2_{\pm.11}$	$83.3_{\pm1.7}$	$91.3_{\pm.24}$	
$\hat{B}_0 A_{rand}$ ($r = 8$)	0.3M	$90.1_{\pm.19}$	$95.8_{\pm.29}$	$89.7_{\pm.13}$	$67.5_{\pm1.2}$	$94.0_{\pm.27}$	$82.8_{\pm1.5}$	$91.9_{\pm.26}$	
$\hat{B}_0 A_{km}$ ($r = 8$)	0.3M	$90.1_{\pm.17}$	$95.6_{\pm.17}$	$90.6_{\pm.32}$	$67.3_{\pm2.3}$	$93.4_{\pm.61}$	$82.4_{\pm1.4}$	$91.2_{\pm.29}$	
$B_U \hat{A}_0$ ($r = 8$)	0.3M	$89.3_{\pm.18}$	$95.4_{\pm0.13}$	$88.8_{\pm0.70}$	$59.1_{\pm0.48}$	$93.8_{\pm0.15}$	$77.5_{\pm2.7}$	$90.7_{\pm.27}$	
$B_{rand} \hat{A}_0$ ($r = 8$)	0.3M	$90.3_{\pm.18}$	$95.5_{\pm.66}$	$89.3_{\pm.09}$	$58.7_{\pm2.5}$	$93.8_{\pm.21}$	$77.1_{\pm1.3}$	$90.7_{\pm.31}$	
$B_{km} \hat{A}_0$ ($r = 8$)	0.3M	$34.5_{\pm1.6}$	$95.2_{\pm.34}$	$89.3_{\pm.11}$	$0.0_{\pm0.0}$	$93.0_{\pm.38}$	$47.3_{\pm.0}$	$91.2_{\pm.24}$	
$\hat{B}_0 A_V$ ($r = 16$)	0.8M	$90.2_{\pm.17}$	$95.8_{\pm.20}$	$90.1_{\pm.56}$	$67.8_{\pm.49}$	$94.5_{\pm.07}$	$82.8_{\pm.42}$	$91.6_{\pm.21}$	
$\hat{B}_0 A_{rand}$ ($r = 16$)	0.8M	$90.1_{\pm.20}$	$96.1_{\pm.18}$	$90.7_{\pm.90}$	$66.1_{\pm2.6}$	$94.4_{\pm.10}$	$84.1_{\pm.96}$	$91.2_{\pm.42}$	
$\hat{B}_0 A_{km}$ ($r = 16$)	0.8M	$90.3_{\pm.06}$	$95.6_{\pm.01}$	$91.1_{\pm.32}$	$65.2_{\pm2.1}$	$94.5_{\pm.02}$	$81.7_{\pm1.8}$	$91.2_{\pm.39}$	
$B_U \hat{A}_0$ ($r = 16$)	0.8M	$90.3_{\pm.07}$	$95.4_{\pm.57}$	$90.4_{\pm1.1}$	$60.7_{\pm.14}$	$94.1_{\pm.30}$	$80.1_{\pm1.2}$	$90.8_{\pm.29}$	
$B_{rand} \hat{A}_0$ ($r = 16$)	0.8M	$89.9_{\pm.19}$	$95.6_{\pm.64}$	$90.2_{\pm0.23}$	$60.3_{\pm3.3}$	$93.9_{\pm0.25}$	$80.4_{\pm0.21}$	$90.9_{\pm0.13}$	
$B_{km} \hat{A}_0$ ($r = 16$)	0.8M	$89.2_{\pm.03}$	$95.2_{\pm.29}$	$90.6_{\pm0.65}$	$40.4_{\pm35.}$	$93.1_{\pm0.23}$	$70.3_{\pm0.19}$	$91.4_{\pm0.26}$	
$\hat{B}_0 \hat{A}_V$ ($r = 8$)	0.8M	$90.4_{\pm.11}$	$95.9_{\pm0.18}$	$90.7_{\pm0.84}$	$64.0_{\pm0.50}$	$94.4_{\pm0.16}$	$84.1_{\pm0.15}$	$91.8_{\pm00.15}$	
$\hat{B}_0 \hat{A}_{rand}$ ($r = 8$)	0.8M	$90.4_{\pm.15}$	$96.0_{\pm.63}$	$91.5_{\pm1.1}$	$64.1_{\pm0.67}$	$94.5_{\pm0.11}$	$85.6_{\pm0.96}$	$92.0_{\pm0.31}$	
$\hat{B}_0 \hat{A}_{km}$ ($r = 8$)	0.8M	$90.3_{\pm.07}$	$95.6_{\pm0.36}$	$90.3_{\pm0.85}$	$64.4_{\pm1.8}$	$94.0_{\pm0.29}$	$84.1_{\pm0.96}$	$91.5_{\pm0.16}$	
$\hat{B}_U \hat{A}_0$ ($r = 8$)	0.8M	$90.3_{\pm.11}$	$96.1_{\pm.18}$	$91.7_{\pm0.33}$	$64.9_{\pm1.5}$	$94.7_{\pm0.33}$	$84.8_{\pm0.96}$	$91.9_{\pm0.19}$	
$\hat{B}_{rand} \hat{A}_0$ ($r = 8$)	0.8M	$90.3_{\pm.27}$	$96.0_{\pm.26}$	$90.8_{\pm0.51}$	$66.0_{\pm1.01}$	$94.5_{\pm0.38}$	$83.6_{\pm1.5}$	$92.0_{\pm0.18}$	
$\hat{B}_{km} \hat{A}_0$ ($r = 8$)	0.8M	$35.5_{\pm1.6}$	$95.6_{\pm.65}$	$90.0_{\pm0.46}$	$21.3_{\pm36.}$	$93.8_{\pm0.01}$	$57.4_{\pm0.17}$	$91.6_{\pm0.43}$	

H Additional language results

See Table 10.

I Additional Vision Transformers and Generalization Results

Table 11 displays a more fine-grained version of Table 7 in the main text and presents results for each out-of-distribution environment independently. Additional results for TerraIncognita, as well as generalization results, can be found in Table 12 and Table 13, respectively. TerraIncognita seems to be a particularly challenging dataset to which low-rank adapters struggle to fit; the most effective method, in this case, appears to be full fine-tuning. In terms of generalization, we can observe that fine-tuning only a single adapter matrix generally results in a lower difference between training set and test set accuracy compared to standard LoRA for all datasets.

Table 11: DomainBed results (mean accuracy and standard deviation in %). ID and OOD denote in-domain and out-of-domain generalization, respectively.

Method	# Trainable Parameters (% full ViT params)	VLCS				PACS				OfficeHome			
		Caltech101 (OOD)	LabelMe (ID)	SUN09 (OOD)	VOC2007 (OOD)	Art (OOD)	Cartoon (ID)	Photo (OOD)	Sketch (OOD)	Art (OOD)	Clipart (ID)	Product (OOD)	Photo (OOD)
$\hat{B}A_{rand}$ $(r=8)$	0.16M-0.2M (0.18-0.29%)	**93.19**$_{\pm 2.27}$	77.40$_{\pm 2.30}$	**61.52**$_{\pm 1.50}$	72.72$_{\pm 1.18}$	81.22$_{\pm 1.40}$	92.45$_{\pm 2.68}$	96.07$_{\pm 0.86}$	40.37$_{\pm 0.83}$	73.59$_{\pm 0.59}$	77.66$_{\pm 0.89}$	78.02$_{\pm 0.14}$	81.55$_{\pm 0.24}$
$\hat{B}A_{rand}$ $(r=16)$	0.3M-0.4M (0.36-0.46%)	91.57$_{\pm 0.81}$	**79.10**$_{\pm 1.41}$	60.97$_{\pm 2.44}$	**73.66**$_{\pm 0.46}$	**84.36**$_{\pm 0.54}$	93.52$_{\pm 0.20}$	**97.07**$_{\pm 0.47}$	39.87$_{\pm 0.99}$	**73.64**$_{\pm 0.40}$	77.63$_{\pm 0.84}$	**78.07**$_{\pm 0.22}$	**81.85**$_{\pm 0.36}$
$B_{rand}\hat{A}$ $(r=8)$	0.16M-0.2M (0.18-0.29%)	87.18$_{\pm 0.77}$	76.71$_{\pm 0.93}$	59.89$_{\pm 1.79}$	70.44$_{\pm 0.10}$	77.05$_{\pm 0.74}$	92.02$_{\pm 1.07}$	92.06$_{\pm 0.34}$	29.65$_{\pm 1.31}$	68.36$_{\pm 0.28}$	72.36$_{\pm 0.69}$	74.00$_{\pm 0.31}$	78.63$_{\pm 0.45}$
$B_{rand}\hat{A}$ $(r=16)$	0.3M-0.4M (0.36-0.46%)	89.28$_{\pm 2.51}$	78.03$_{\pm 1.23}$	60.44$_{\pm 1.84}$	70.81$_{\pm 0.36}$	81.43$_{\pm 0.92}$	93.87$_{\pm 0.73}$	95.63$_{\pm 0.13}$	35.02$_{\pm 0.86}$	71.64$_{\pm 0.24}$	73.77$_{\pm 1.13}$	75.46$_{\pm 0.25}$	80.31$_{\pm 0.39}$
LoRA $(r=8)$	0.3M-0.4M (0.35-0.46%)	44.59$_{\pm 1.96}$	73.51$_{\pm 0.62}$	60.44$_{\pm 2.86}$	64.26$_{\pm 1.07}$	81.41$_{\pm 0.70}$	**94.94**$_{\pm 0.56}$	95.43$_{\pm 0.54}$	49.90$_{\pm 1.51}$	70.44$_{\pm 0.46}$	78.54$_{\pm 1.49}$	73.99$_{\pm 0.64}$	78.95$_{\pm 0.10}$
Linear Probing	0.004M (0.00%)	90.65$_{\pm 2.51}$	75.58$_{\pm 1.66}$	53.74$_{\pm 0.27}$	70.71$_{\pm 0.35}$	67.66$_{\pm 0.63}$	81.62$_{\pm 0.34}$	88.80$_{\pm 1.43}$	28.72$_{\pm 1.70}$	64.56$_{\pm 0.23}$	58.38$_{\pm 0.76}$	66.97$_{\pm 0.43}$	74.23$_{\pm .001}$
Full FT	86.4M (100%)	70.57$_{\pm 15.13}$	76.21$_{\pm 1.95}$	57.14$_{\pm 1.46}$	66.90$_{\pm 2.72}$	75.52$_{\pm 2.89}$	98.15$_{\pm 0.56}$	89.54$_{\pm 1.88}$	**59.63**$_{\pm 2.53}$	58.38$_{\pm 0.64}$	**80.67**$_{\pm 1.22}$	63.05$_{\pm 0.85}$	68.27$_{\pm 0.43}$

Table 12: TerraIncognita results (mean accuracy and standard deviation in %). All methods were trained for 20,000 steps.

Method	# Trainable Parameters (% full ViT params)	TerraIncognita L100 (OOD)	L38 (ID)	L43 (OOD)	L46 (OOD)
$\hat{B}A_{rand}$ $(r=8)$	0.16M-0.2M (0.18-0.29%)	16.59$_{\pm 2.59}$	79.88$_{\pm 0.45}$	6.46$_{\pm 1.25}$	10.96$_{\pm 0.52}$
$\hat{B}A_{rand}$ $(r=16)$	0.3M-0.4M (0.36-0.46%)	14.14$_{\pm 1.45}$	80.48$_{\pm 0.99}$	7.74$_{\pm 0.26}$	11.09$_{\pm 0.76}$
$B_{rand}\hat{A}$ $(r=8)$	0.16M-0.2M (0.18-0.29%)	12.82$_{\pm 0.84}$	78.65$_{\pm 0.57}$	3.42$_{\pm 0.81}$	7.24$_{\pm 1.36}$
$B_{rand}\hat{A}$ $(r=16)$	0.3M-0.4M (0.36-0.46%)	17.58$_{\pm 1.01}$	78.89$_{\pm 0.55}$	8.41$_{\pm 1.88}$	7.62$_{\pm 0.56}$
LoRA $(r=8)$	0.3M-0.4M (0.35-0.46%)	**41.36**$_{\pm 2.94}$	87.33$_{\pm .13}$	13.48$_{\pm 2.19}$	7.76$_{\pm 1.69}$
Linear Probing	0.004M (0.00%)	13.82$_{\pm .20}$	69.82$_{\pm 0.36}$	10.06$_{\pm .45}$	13.90$_{\pm .49}$
Full FT	86.4M (100%)	38.33$_{\pm 6.50}$	**95.05**$_{\pm .31}$	**14.18**$_{\pm 2.33}$	**19.50**$_{\pm 1.53}$

Table 13: Generalization results (train set - test set accuracy in %) for DomainBed.

Method	# Trainable Parameters (% full ViT params)	VLCS				PACS				OfficeHome				TerraIncognita			
		Caltech101 (OOD)	LabelMe (ID)	SUN09 (OOD)	VOC2007 (OOD)	Art (OOD)	Cartoon (ID)	Photo (OOD)	Sketch (OOD)	Art (OOD)	Clipart (ID)	Product (OOD)	Photo (OOD)	L100 (OOD)	L38 (ID)	L43 (OOD)	L46 (OOD)
$\hat{B}A_{rand}$ $(r=8)$	0.2M-M (0.29-0.%)	-1.72$_{\pm 2.24}$	11.82$_{\pm 1.21}$	28.09$_{\pm 2.04}$	16.98$_{\pm 0.74}$	15.82$_{\pm 0.68}$	3.83$_{\pm 0.70}$	0.83$_{\pm 0.30}$	57.34$_{\pm 0.89}$	15.94$_{\pm 0.28}$	11.87$_{\pm 1.14}$	11.51$_{\pm 0.47}$	7.97$_{\pm 0.56}$	64.20$_{\pm 2.58}$	0.91$_{\pm 0.43}$	74.33$_{\pm 1.26}$	69.82$_{\pm 0.53}$
$\hat{B}A_{rand}$ $(r=16)$	0.3M-0.4M (0.36-0.46%)	-2.48$_{\pm 0.69}$	9.99$_{\pm 1.44}$	28.11$_{\pm 2.74}$	15.43$_{\pm 0.70}$	12.92$_{\pm 0.87}$	3.76$_{\pm 0.40}$	0.22$_{\pm 0.67}$	57.42$_{\pm 0.62}$	16.22$_{\pm 0.93}$	12.25$_{\pm 1.23}$	11.81$_{\pm 0.34}$	8.19$_{\pm 0.87}$	66.62$_{\pm 1.54}$	0.28$_{\pm 1.18}$	73.02$_{\pm 0.24}$	69.67$_{\pm 0.56}$
$B_{rand}\hat{A}$ $(r=8)$	0.2M-M (0.29-0.%)	0.19$_{\pm 0.86}$	10.66$_{\pm 0.86}$	27.48$_{\pm 1.86}$	16.93$_{\pm 0.19}$	19.79$_{\pm 0.66}$	4.81$_{\pm 0.99}$	4.78$_{\pm 0.29}$	67.19$_{\pm 1.34}$	17.73$_{\pm 0.30}$	13.73$_{\pm 0.86}$	12.08$_{\pm 0.42}$	7.45$_{\pm 0.65}$	65.86$_{\pm 0.64}$	0.04$_{\pm 0.60}$	75.27$_{\pm 0.50}$	71.45$_{\pm 1.17}$
$B_{rand}\hat{A}$ $(r=16)$	0.3M-0.4M (0.36-0.46%)	-1.50$_{\pm 2.88}$	9.75$_{\pm 0.85}$	27.34$_{\pm 2.07}$	16.97$_{\pm 0.61}$	15.89$_{\pm 0.96}$	3.44$_{\pm 0.54}$	1.69$_{\pm 0.30}$	62.30$_{\pm 0.83}$	15.20$_{\pm 0.53}$	13.07$_{\pm 1.30}$	11.38$_{\pm 0.38}$	6.53$_{\pm 0.64}$	62.17$_{\pm 1.41}$	0.86$_{\pm 0.96}$	71.34$_{\pm 1.91}$	72.13$_{\pm 0.15}$
LoRA $(r=8)$	0.3M-0.4M (0.35-0.46%)	52.94$_{\pm 1.48}$	24.03$_{\pm 0.16}$	37.10$_{\pm 3.25}$	33.28$_{\pm 1.64}$	18.23$_{\pm 0.74}$	4.70$_{\pm 0.57}$	4.22$_{\pm 0.43}$	49.74$_{\pm 1.44}$	26.07$_{\pm 0.39}$	17.97$_{\pm 1.80}$	22.53$_{\pm 0.63}$	17.57$_{\pm 0.23}$	47.53$_{\pm 2.80}$	1.56$_{\pm 0.24}$	75.41$_{\pm 2.29}$	81.12$_{\pm 1.73}$
Linear Probing	0.004M (0.00%)	-12.03$_{\pm 2.11}$	3.04$_{\pm 1.38}$	24.88$_{\pm 0.47}$	7.91$_{\pm 0.79}$	17.18$_{\pm 0.13}$	3.22$_{\pm 0.40}$	-3.96$_{\pm 1.90}$	56.13$_{\pm 1.33}$	6.02$_{\pm 0.21}$	12.20$_{\pm 1.03}$	3.61$_{\pm 0.51}$	-3.65$_{\pm 0.19}$	55.17$_{\pm 0.28}$	-0.82$_{\pm 0.31}$	58.94$_{\pm 0.52}$	55.10$_{\pm 0.52}$
Full FT	86.4M (100%)	29.03$_{\pm 15.27}$	23.40$_{\pm 2.05}$	42.47$_{\pm 1.83}$	32.70$_{\pm 2.27}$	24.41$_{\pm 2.94}$	1.78$_{\pm 0.54}$	10.38$_{\pm 1.90}$	40.30$_{\pm 2.49}$	40.23$_{\pm 0.48}$	17.94$_{\pm 1.36}$	35.56$_{\pm 1.02}$	30.35$_{\pm 0.53}$	59.84$_{\pm 6.53}$	3.12$_{\pm 0.26}$	83.99$_{\pm 2.31}$	78.67$_{\pm 1.47}$